MASS DEPENDENCE OF THE SLOPES: COMPARISON OF DIFFERENT PARAMETRIZATIONS, OBSERVATION OF REGULARITIES IN THE DATA

By A. Guła

Institute of Nuclear Technology, Academy of Mining and Metallurgy, Cracow*

(*Received July 18, 1973; Revised paper received October 23, 1973*)

The mass dependence of the slopes in hadronic production processes is analysed. Different parametrizations of the data are compared. A parametrization is found which describes very well the data for processes of different kinds (exclusive: diffractive and non-diffractive, and inclusive) and which exhibits some interesting regularities in the data. In particular the slopes in production processes at large invariant masses of the produced system of particles are related to the slopes in two-body and quasi-two body reactions. The slopes for meson resonances produced in nondiffractive processes are found to deviate from a smooth slope-versus-mass dependence of the background in a way depending on the Q-value of the resonance.

1. *Introduction*

As in the two-body and quasi two-body reactions, the differential cross-sections in production processes exhibit forward peaks at small values of the invariant four-momentum transfer variable $|t'|$ (the notation is explained in Fig. 1)[1]. These peaks, in general, can be well parametrized by a single exponential in t':

$$\frac{d\sigma}{dt'} = ae^{bt'}, \tag{1}$$

at least in some interval near the forward direction (usually $0.05 < -t' < 0.5$ (GeV/c)^2). Parameter b in Eq. (1) determines the slope of the forward peak.

It follows from many experiments [1–8, 22–26] that in production processes the slopes of the forward peaks depend on the mass M of the produced system of particles (S in Fig. 1): the larger the mass, the smaller is, in general, the slope of the forward peak.

* Address: Akademia Górniczo-Hutnicza, Instytut Techniki Jądrowej, Al. Mickiewicza 30, 30-059 Kraków, Poland.

[1] As usual, $t' = t - t_{\min}$, where $t_{\min}$ is the value of the invariant four-momentum transfer t, corresponding to the production of mass M in the forward direction.

This phenomenon has been observed both in inclusive (*e.g.* [4, 8, 26]) and exclusive (*e.g.* [1–3, 4–7, 22–25]) reactions, and in the latter case, both in diffractive and non-diffractive channels, and it seems to be a feature common to all production processes.

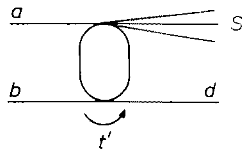

Fig. 1. Diagram explaining the notation

There exist now quite numerous data on the mass dependence of the slopes of the forward peaks. It is therefore tempting to try to find a parametrization of the data which would be valid for different kinds of processes and to scan the data for possibly existing regularities.

TABLE I

Description of the experimental data

No.	Process	p_{lab} GeV/c	Mass GeV		$-t'$ (GeV/c)^2		p_{cut} GeV/c	Threshold	Numbers of points		Points omitted
			min	max	min	max			all	cut	
1	$\pi^+p \to (\pi^+\pi^+\pi^-)p$	16.0	0.6	3.0			1.7[a]	$\pi\pi\pi$	4	4	A_2
2	$\pi^+p \to (\pi^+\pi^+\pi^-)p$[b]	8.0	0.5	2.4	0	0.4	1.0	$\pi\pi\pi$	7	6	A_2
3	$\pi^-p \to (\pi^-\pi^-\pi^+)p$	16.0	0.5	3.5	0.02	0.6	1.5[a]	$\pi\pi\pi$	7	7	A_2
4	$K^-p \to (K^-\pi^+\pi^-)p$	10.1	1.0	2.5	0	0.4	1.3	$K\pi\pi$	8	7	Q
5	$K^-p \to (\bar{K}^0\pi^-)p$	10.1	0.6	2.5	0.05	0.6	1.3	$K\pi$	8	7	K^*
6	$K^-p \to (K^-\pi^+)n$	10.1	0.6	2.5	0	0.6	1.3	$K\pi$	8	7	K^*
7	$K^-p \to (\bar{K}^0\pi^-)\Delta^+$	10.1	0.6	2.5	0	0.6	1.2	$K\pi$	6	5	K^*
8	$K^-p \to (K^-\pi^+)\Delta^0$	10.1	0.6	2.5	0	0.6	1.2	$K\pi$	6	5	K^*
9	$\pi^+p \to (\pi^+\pi^-)\Delta^{++}$	8.0	0.5	2.0	0	0.4	1.1	$\pi\pi$	7	6	f^0
10	$\pi^+p \to (\pi^+\pi^0\pi^-)\Delta^{++}$	8.0	0.9	1.8	0	0.4	1.4	$\pi\pi\pi$	7	4	ω,η
11	$\pi^+p \to \pi_f^+(\pi^+\pi^-p)$	16.0	1.2	3.2			2.1[a]	$\pi\pi p$	5	5	—
12	$\pi^+p \to \pi_f(\pi N)_{I=1/2}$	8.0	1.1	2.3	0	0.6	1.4	πp	6	5	—
13	$\pi^-p \to \pi^-(\pi^+\pi^-p)$	16.0	1.2	3.5	0	0.6	2.0[a]	$\pi\pi p$	5	5	—
14	$\pi^-p \to \pi^-(\pi^+n)$	11.0	1.3	3.1			1.5[a]	πn	8	8	—
15	$K^-p \to$ (pions) Λ^0	10.1	0.7	2.8	0	0.5	1.0	4π	12	7	—
16	$K^\pm p \to K^0X$	8.10	1.8	3.0	0	1.0	1	πp	23	13	—
17	$K^-p \to \bar{K}^0X^0$	10.1	1.8	3.2	0	1.0	1.0	πp	21	14	—
18	$K^+p \to K^0X^{++}$	8.2	1.8	2.9	0	1.0	0.9	πp	18	11	—
19	$\pi^+p \to \pi^0(\pi^+p)$	8.0	1.1	3.0	0	0.4	1.0	πp	7	7	—
20	$\pi^+p \to \pi_f^0(\pi^+p)$[c]	8.0	1.1	2.3	0	0.6	1.4	πp	6	5	—
21	$\gamma p \to (\pi^+\pi^-)p$	9.5	0.3	2.0	0.5	0.5	1.2	$\pi\pi$	24	24	—
22	$pp \to pX^+$	28.5	1.3	2.1	0.08	0.16	3.4[a]	$\pi\pi p$	3	3	$N^*(1.4)$
23	$pp \to p(\pi^+n)$	28.5	1.1	1.9	0	0.2–0.6	3.4[a]	πn	3	3	$N^*(1.4)$
24	$pp \to p(\pi^-\Delta^{++})$	28.5	1.4	2.1	0	0.2–0.4	3.4[a]	$\pi\Delta$	3	3	$N^*(1.4)$
25	$pp \to p(\pi^-\Delta^{++})$	19.2	1.4	2.0	0	0.5	3.0[a]	$\pi\Delta$	9	9	$N^*(1.4)$

[a] Data terminate at this value. [b] Δ^{++} excluded. [c] $M(\pi\pi) \geqslant 0.86$ GeV.

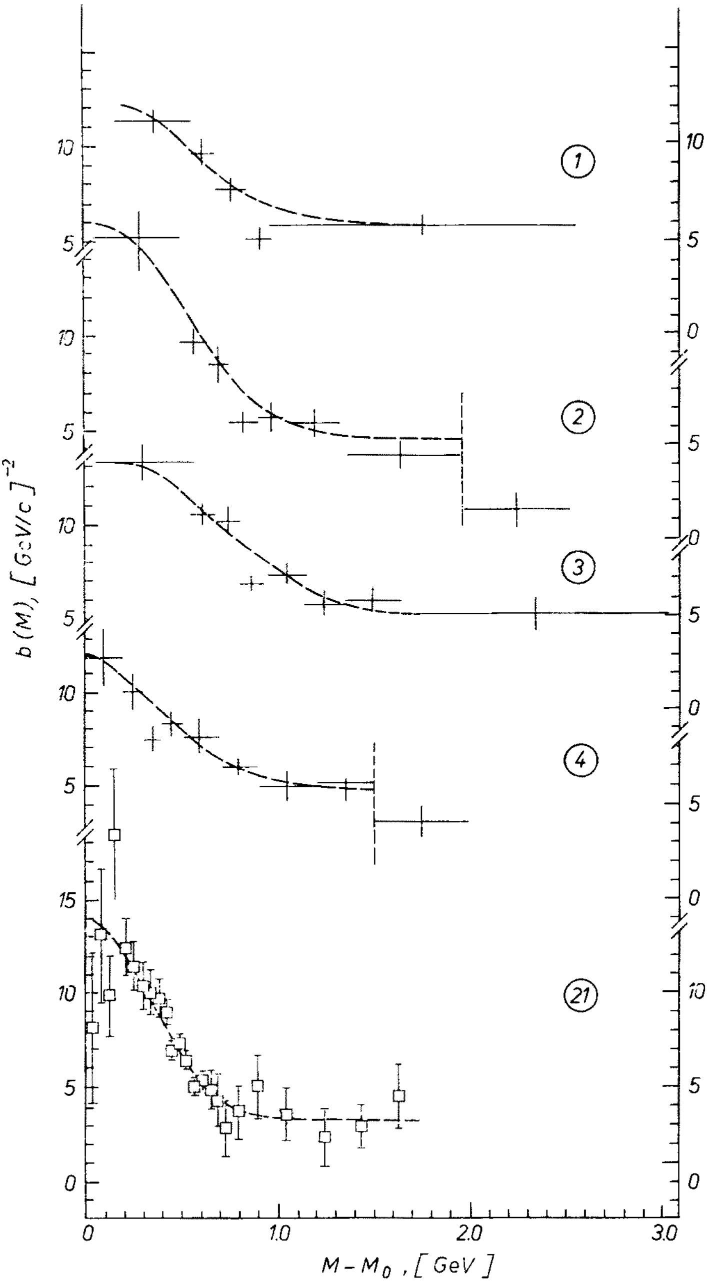

Fig. 2a

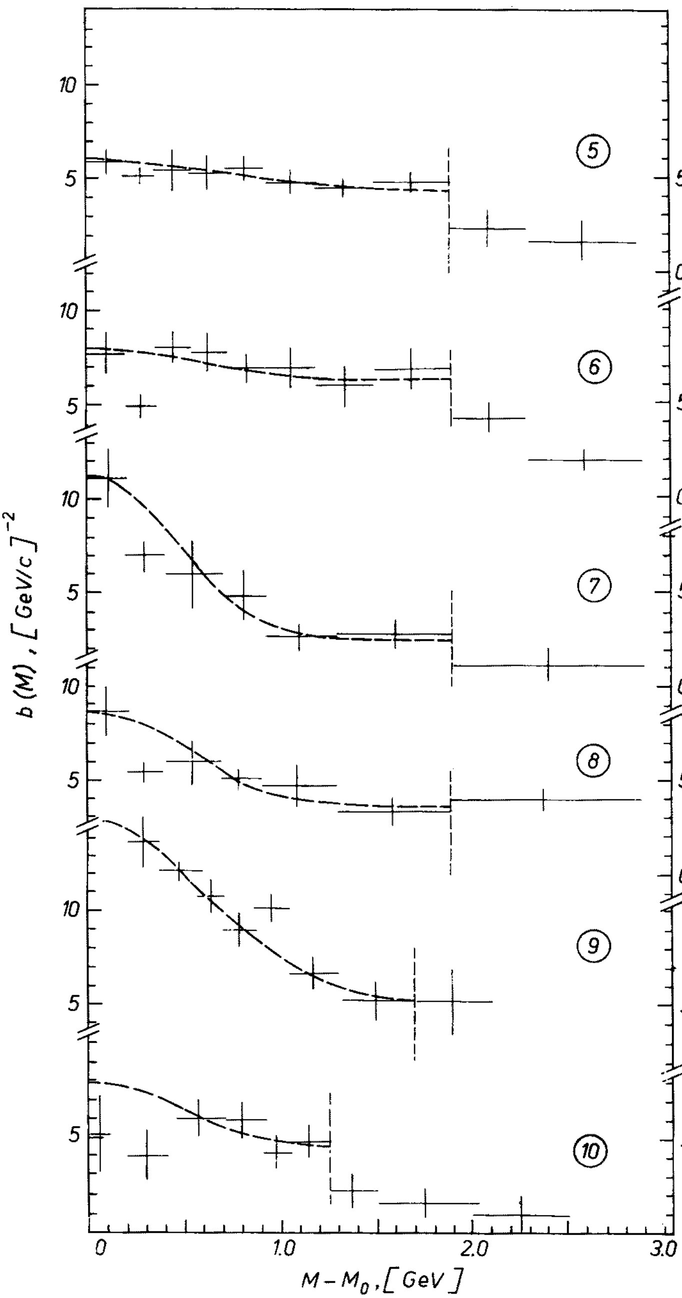

Fig. 2b

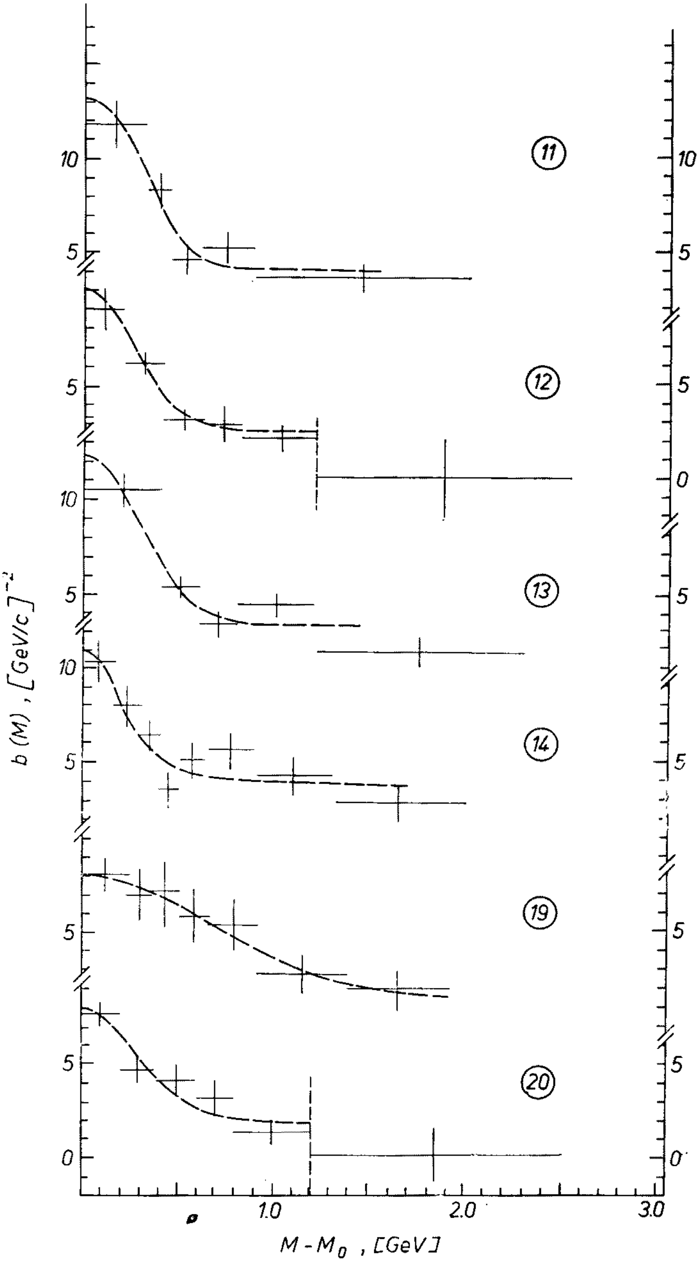

Fig. 2c

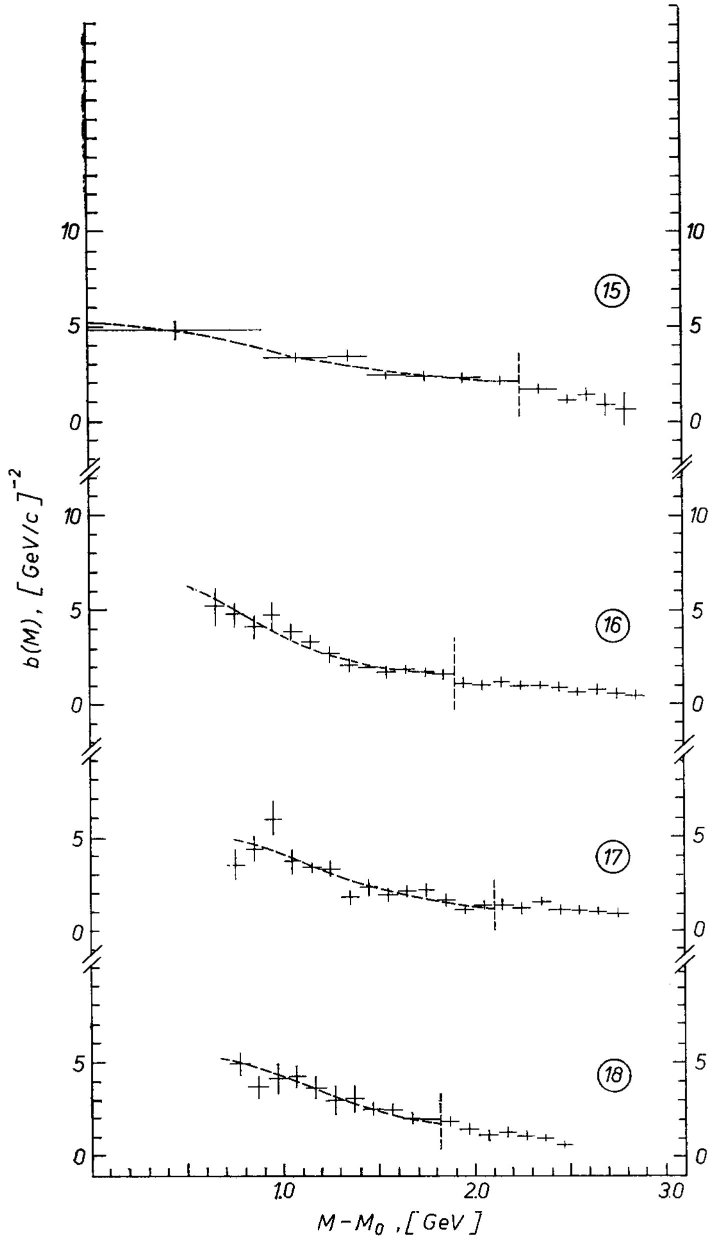

Fig. 2d

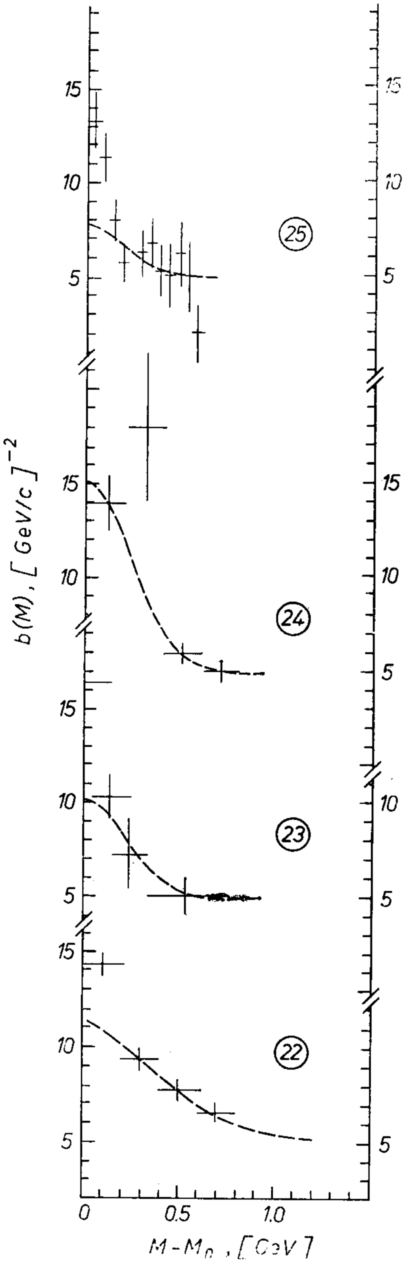

Fig. 2e

Fig. 2. Mass dependence of the slopes in production processes. Horizontal axis represents the mass of system S in Fig. 1 minus the threshold mass for this system. The vertical axis represents the slope parameter of the forward peak. Numbers at the curves correspond to the ordering of processes in Table I. Solid lines are the best-fit curves obtained using parametrization (2e). The dashed vertical lines indicate the cut-off masses described in text

In this work the data on the mass dependence of the slopes of the forward peaks have been analysed for 23 different processes, some of them at different energies. A short account of this work has been published earlier [17].

The data analysed in this paper are described in Table I and shown in Figs 2a–2e. As it is seen from the figures, the slope decreases, in general monotonically, with increasing mass of the produced system of particles. The deviations from the smooth slope--versus-mass dependence, which appear at several masses, seem to be particularly significant at the masses corresponding to resonances in system S (K^*, f^0, A_2 and Q).

2. *Slopes at large masses*

From the point of view of the models which predict the mass dependence of the slopes, it is particularly interesting to consider the processes in which all the particles belonging to system S are produced in one of the vertices in Fig. 1. At low masses of system S the admixture of events in which some of the particles belonging to this system are produced at the other vertex can be expected to be small. On the other hand, at higher masses this admixture can become quite significant, if peripheral production at the other vertex is abundant. Therefore, in this work the points at the masses close to the high-mass kinematical limits have been treated separately. The vertical dashed lines in Figs 2a–2e indicate the masses corresponding to the center-of-mass momenta of particle d in the final state (see Fig. 1) of about $p_{\mathrm{cut}} \approx 1$ GeV/c. The points on the right-hand sides of these lines have not been considered in this analysis in those cases in which the physical picture behind a formula implied that all particles in system S should be associated with one vertex. More accurate values of the cut-off momenta p_{cut} corresponding to the end-points of the mass intervals in which slopes have been determined are given in Table I.

If one is looking only at the points on the left-hand sides of the cut-off vertical dashed lines, the data in Figs 2a–2e suggest that the slope parameter of the forward peak in a given process tends with increasing mass to a positive limit b_0, which is characteristic for the vertex at which production does not take place (this vertex will be referred to as "nonproduction" vertex, in the following). For the processes in which the "nonproduction" vertex in Fig. 1 is a baryonic vertex, b_0 is, in general, about 4–5 (GeV/c)$^{-2}$, whereas — if it is a mesonic vertex — b_0 assumes, in general, smaller values: $b_0 \approx 1-4$ (GeV/c)$^{-2}$.

There exist some theoretical indications for such a behaviour of the slopes with increasing mass of the produced system [16, 27–29]. In particular, Satz [16] has proposed a model for diffractive processes according to which the slope parameter at large masses of a diffractively produced system is determined by the form-factor of the vertex at which production does not occur: *e.g.*, if b and d in Fig. 1 denote protons, then: $b_0 = 1/2$ $b(\mathrm{pp} \to \mathrm{pp}) \approx 5$ (GeV/c)$^{-2}$. Similar behaviour, also for diffractive processes, has been predicted from the Glauber theory by Trefil [27] who found that for masses past the resonance region the slope is primarily determined by the radius of the object (particle or nucleus) which remains intact in the collision. For nondiffractive processes such a behaviour of the slope at large masses can be expected from the multi-regge model of Caneschi [28] (formula (2d) below). The same prediction has been obtained in the tripple-regge limit for inclusive processes [29]. In all the models mentioned above the particles belonging to system S can be associated with one vertex in Fig. 1. As it is seen in Figs 2a–2e the slope parameter in a given process indeed approaches some positive limit, at least when masses corresponding to c.m. momenta of particle d in Fig. 1 greater than $p_{cut} \approx 1$ GeV/c are considered.

3. *Parametrization of the data*

a) Description of formulae

In order to find a parametrization which would describe the mass dependence of the slopes in different kinds of processes, several formulae have been tried:

$$b(M) = b_0 + b_1 M^{-\alpha}, \tag{2a}$$

$$b(M) = b_1 \frac{s - M^2}{s}, \tag{2b}$$

$$b(M) = 2\alpha' \ln\left(1 + \frac{s}{M^2}\right), \tag{2c}$$

$$b(M) = b_0 + 2\alpha' \ln\left(\frac{s}{M^2}\right), \tag{2d}$$

$$b(M) = b_0 + b_1 \exp\left[-\frac{(M - M_0)^2}{2d^2}\right]. \tag{2e}$$

Parametrization (2a) with $b_0 = 0$ has been used as an empirical formula in references [1–4]. In this paper also the possibility: $b_0 \neq 0$ is considered, in order to take into account the tendency displayed by the data. Free parameters in Eq. (2a) are: b_0, b_1, and α. Formula (2b) was derived by Muirhead [18] on the basis of simple kinematical considerations, in which the decrease of the slope parameter had been attributed to the decrease of the available relative angular momentum in system $S-d$ in Fig. 1 with increasing invariant mass of the produced system of particles S. In Eq. (2b), s denotes the square of the total s-channel c.m. energy; b_1 is a free parameter. Equation (2c) was derived in the statistical approach to the Veneziano model [30]. Here, α' denotes the slope of a Regge trajectory (typically $\alpha' \approx 1$ (GeV/c)$^{-2}$ for nonvacuum exchanges). Numerically similar behaviour of slope has been found in the thermodynamic model [31]. In this analysis equation (2c) was considered as an alternative parametrization of the data and α' was treated as a free parameter. Formula (2d) has been obtained in the multi-regge model of Caneschi [28]. The same expression for the slope as a function of mass follows from the tripple-regge approach [29] and from the Veneziano model applied to inclusive processes [32]. In the fits presented in this paper α' has been restricted by imposing the condition: $\alpha' \leqslant 1.0$ (GeV/c)$^{-2}$. Another fitted parameter in equation (2d) is b_0. Parametrization (2e) has been proposed in Ref. [23] where it has also been found that interesting regularities are present among the parameters of equation (2e) for different processes (see the next section). M_0 denotes in equation (2e) the threshold mass of system S in Fig. 1; b_0, b_1 and d are free parameters. The thresholds M_0 used in the fits presented below are listed in Table I.

b) Data selection

As mentioned in Section 2, the masses corresponding to c.m. momenta of particle d in Fig. 1 smaller than $p_{cut} = 1$ GeV/c, have been treated separately in the fits. In those cases where the physical picture on which the formula is based is such that all the particles belonging to system S should be associated with one of the vertices in Fig. 1, the points at masses corresponding to $p_d < p_{cut}$ have not been taken into account in the calculations. Such a procedure provides a (very) rough selection of events in which production takes place at one vertex, by rejecting those interactions in which some of the particles in system S have been produced peripherally at the other vertex. The cut-off masses and the corresponding c.m. momenta p_{cut} are listed in Table I.

In order to secure large enough mass intervals between the thresholds and cut-off masses, the analysis has been confined to processes at $p_{lab} \geqslant 8$ GeV/c.[2]

The data on proton-proton collisions at 19.2 and 28.5 GeV/c have been treated in this analysis in a slightly different way: Since the mass intervals, in which the determination of slopes has been done in these processes, span only about 0.5–0.8 GeV (see Fig. 2e), the values of parameters b_0 cannot be determined reliably by fitting the data in Fig. 2e. Therefore, for these proton-proton processes the fits were performed assuming b_0 to be half the elastic proton-proton slope in this energy range: $b_0 = 5$ (GeV/c)$^{-2}$. As mentioned earlier, this value is suggested by some models, *e.g.* by the Satz model for diffractive processes [16].

Since resonance production mechanism may be quite different from that through which the neighbouring background is produced, one can expect deviations from a smooth slope-versus-mass dependence at the masses corresponding to resonances in system S. Therefore the points corresponding to resonance masses at which the slope parameter deviates significantly from the smooth extrapolation through the neighbouring points, have not been taken into account in the fits presented in this paper. The omitted points are indicated in Table I. The points corresponding to the remaining resonances, at which no significant deviations occur, have been included in the calculations. It has been checked that the omission of these points does not influence significantly the results.

c) Results of the fits

Parametrizations (2a)–(2e) are compared in Table II which contains the cumulative χ^2-values for all the processes 1–21 in Table II together with the corresponding χ^2 probabilities. Table III contains the values of some of the parameters entering equations (2a)–(2d). The values of the parameters of equation (2e) are listed in Table IV.

---

[2] Obviously, due to the errors of the experimental points, the behaviour of the slope parameter at masses close to the threshold mass M_0 does not determine the behaviour of the slope parameter at large masses. At $p_{lab} < 8$ GeV/c the cut-off applied in this analysis ($p_{cut} \approx 1$ GeV/c) corresponds to masses close to M_0 and no reliable information about the limits b_0 can be obtained by fitting the data.

TABLE II

Comparison of parametrizations (2a)–(2e)

Formula	Cut-off	Comment	χ^2	N	DF	N/DF	P(χ^2)
(2a)	without	$b_0 = 0$	243.1	205	163	1.49	1%
(2a)	with	$b_0 = 0$	157.4	162	120	1.31	3%
(2a)	with	$b_0 =$ fit	136.0	162	99	1.37	1%
(2b)	without	—	1058.1	205	184	5.75	<0.5%
(2b)	with	—	868.8	162	141	6.16	<0.5%
(2c)	with	$\alpha' =$ fit	485.5	162	141	3.44	<0.5%
(2d)	with	$0.7 < \alpha' < 1$	431.8	162	120	3.59	<0.5%
(2e)	with	—	94.3	162	99	0.95	65%

TABLE III

Parameters of Eqs (2a), (2c) and (2d)

		formula (2a)			formula (2c)	formula (2d)	
	Process	b_0(GeV/c)$^{-2}$	b_1(GeV/c)$^{-2}$	α	α'(GeV/c)$^{-2}$	b_0(GeV/c)$^{-2}$	α'(GeV/c)$^{-2}$
1	$\pi^+p \to (\pi^+\pi^+\pi^-)p$	4.8 ± 0.3	4.3 ± 0.6	1.9 ± 0.8	1.40 ± 0.05	2.3 ± 0.3	1.0
2	$\pi^+p \to (\pi^+\pi^+\pi^-)p$	2.7 ± 1.3	7.5 ± 1.6	1.9 ± 0.5	1.65 ± 0.09	2.9 ± 0.5	1.0
3	$\pi^-p \to (\pi^-\pi^-\pi^+)p$	0.8 ± 0.5	10.1 ± 0.4	$1.0\to0.1$	1.46 ± 0.06	2.6 ± 0.2	1.0
4	$K^-p \to (K^-\pi^+\pi^-)p$	0.6 ± 0.3	13.7 ± 2.0	1.4 ± 0.4	1.69 ± 0.11	3.0 ± 0.5	1.0
5	$K^-p \to (\bar{K}^0\pi^-)p$	0.3 ± 1.1	5.3 ± 0.8	0.2 ± 0.1	1.09 ± 0.06	2.2 ± 0.2	0.70 ± 0.01
6	$K^-p \to (K^-\pi^+)n$	0.2 ± 0.3	7.4 ± 0.6	0.2 ± 0.1	1.39 ± 0.12	3.8 ± 0.4	0.71 ± 0.03
7	$K^-p \to (\bar{K}^0\pi^-)\Delta^+$	1.1 ± 0.6	5.5 ± 0.3	1.8 ± 0.5	0.94 ± 0.20	-3.3 ± 0.8	1.0
8	$K^-p \to (K^-\pi^+)\Delta^0$	-2.3 ± 1.7	8.9 ± 2.1	0.6 ± 0.1	1.06 ± 0.12	0.5 ± 0.5	1.0
9	$\pi^+p \to (\pi^+\pi^-)\Delta^{++}$	-0.2 ± 0.4	9.7 ± 0.6	0.8 ± 0.1	1.77 ± 0.09	4.4 ± 0.5	1.0
10	$\pi^+p \to (\pi^+\pi^0\pi^-)\Delta^{++}$	2.0 ± 0.2	4.5 ± 1.9	1.2 ± 1.2	1.14 ± 0.16	1.9 ± 1.2	0.77 ± 0.31
11	$\pi^+p \to \pi_f^+(\pi^+\pi^-p)$	3.4 ± 0.6	43.4 ± 12	5.3 ± 1.2	1.31 ± 0.06	1.5 ± 0.5	1.0
12	$\pi^\pm p \to \pi_f(\pi N)_{I=1/2}$	1.2 ± 0.5	18.5 ± 3.7	4.2 ± 0.6	1.17 ± 0.22	0.8 ± 0.4	1.0
13	$\pi^-p \to \pi^-(\pi^+\pi^-p)$	2.7 ± 0.6	49.5 ± 16	5.5 ± 0.8	1.10 ± 0.10	0.6 ± 0.4	1.0
14	$\pi^-p \to \pi^-(\pi^+n)$	3.9 ± 0.6	14.3 ± 5.4	4.7 ± 1.4	1.10 ± 0.05	1.9 ± 0.4	1.0
15	$K^-p \to$ (pions) Λ^0	-0.5 ± 1.2	5.5 ± 1.4	0.8 ± 0.3	0.71 ± 0.02	0.3 ± 0.2	0.72 ± 0.03
16	$K^+p \to K^0X$	0.1 ± 0.3	23.8 ± 3.0	2.5 ± 0.1	0.93 ± 0.05	0.4 ± 0.1	1.0
17	$K^-p \to \bar{K}^0X^0$	-0.8 ± 0.6	22.0 ± 7.0	2.0 ± 0.5	0.83 ± 0.04	0.2 ± 0.1	1.0
18	$K^+p \to K^0X^{++}$	-2.8 ± 0.9	16.0 ± 3.8	1.2 ± 0.1	1.04 ± 0.06	0.7 ± 0.1	1.0
19	$\pi^+p \to \pi^0(\pi^+p)$	-1.3 ± 2.5	11.7 ± 1.3	1.1 ± 0.8	1.37 ± 0.17	2.0 ± 0.1	1.0
20	$\pi^+p \to \pi_f^0(\pi^+p)$	0.0 ± 0.3	12.1 ± 1.0	2.5 ± 0.5	1.24 ± 0.16	1.1 ± 0.4	1.0
21	$\gamma p \to (\pi^+\pi^-)p$	-0.1 ± 0.1	4.9 ± 0.4	1.1 ± 0.2	1.00 ± 0.06	-0.1 ± 0.2	1.0

It can be seen from Table II that the overall best-fit is obtained for parametrization (2e) which also gives good χ^2-values in the majority of cases. The cumulative χ^2 probability for formula (2a) is much smaller, although the fits for separate processes are, in general, of a comparable quality. On the other hand, the fits obtained using formulae (2b), (2c) and

TABLE IV

Parameters and χ^2-values for Eq. (2e)

	Process	χ^2	b_0 (GeV/c)$^{-2}$	b_1 (GeV/c)$^{-2}$	d (GeV)	R (fm)
1	$\pi^+p \to (\pi^+\pi^+\pi^-)p$	1.0	5.7±0.3	7.6±0.9	0.50±0.09	1.10±0.07
2	$\pi^+p \to (\pi^+\pi^+\pi^-)p$	0.5	4.8±0.8	13.5±2.3	0.46±0.07	1.47±0.13
3	$\pi^-p \to (\pi^-\pi^-\pi^+)p$	2.2	5.4±0.7	9.1±0.5	0.61±0.09	1.21±0.33
4	$K^-p \to (K^-\pi^+\pi^-)p$	0.4	4.9±0.8	8.3±1.2	0.52±0.10	1.15±0.83
5	$K^-p \to (\bar{K}^0\pi^-)p$	1.6	4.7±0.3	1.2±0.7	0.61±0.25	0.44±0.13
6	$K^-p \to (K^-\pi^+)n$	1.1	6.3±0.9	1.8±0.8	0.59±0.35	0.54±0.20
7	$K^-p \to (\bar{K}^0\pi^-)\Delta^+$	0.7	2.4±0.7	8.6±1.7	0.43±0.09	1.17±0.12
8	$K^-p \to (K^-\pi^+)\Delta^0$	0.6	3.4±0.8	4.8±1.1	0.53±0.16	0.88±0.10
9	$\pi^+p \to (\pi^+\pi^-)\Delta^{++}$	0.2	4.7±1.4	10.0±1.7	0.64±0.15	1.26±0.11
10	$\pi^+p \to (\pi^+\pi^0\pi^-)\Delta^{++}$	1.0	4.4±1.5	3.5±1.2	0.46±0.05	0.75±0.13
11	$\pi^+p \to \pi_f^+(\pi^+\pi^-p)$	4.3	4.1±0.3	9.7±2.7	0.25±0.06	1.24±0.17
12	$\pi^+p \to \pi_f(\pi N)_{I=1/2}$	0.9	2.3±0.5	7.9±1.4	0.27±0.03	1.12±0.10
13	$\pi^-p \to \pi^-(\pi^+\pi^-p)$	7.9	3.4±0.4	8.9±1.9	0.27±0.04	1.19±0.11
14	$\pi^-p \to \pi^-(\pi^+n)$	8.1	4.5±0.5	6.9±1.3	0.22±0.04	1.05±0.10
15	$K^-p \to$ (pions) Λ^0	4.6	1.8±0.2	3.4±0.5	0.86±0.10	0.74±0.06
16	$K^\pm p \to K^0X$	6.5	1.6±0.3	6.6±0.7	0.69±0.09	1.03±0.05
17	$K^-p \to \bar{K}^0X^0$	23.3	0.9±0.3	5.8±1.1	0.89±0.09	0.96±0.09
18	$K^+p \to K^0X^{++}$	3.9	0.5±1.1	5.9±2.0	0.86±0.20	0.98±0.17
19	$\pi^+p \to \pi^0(\pi^+p)$	0.4	1.8±1.5	6.3±1.9	0.69±0.23	1.00±0.15
20	$\pi^+p \to \pi_f^0(\pi^+p)$	4.5	2.0±0.8	5.9±1.1	0.31±0.08	0.98±0.09
21	$\gamma p \to (\pi^+\pi^-)p$	20.6	3.7±0.7	10.3±1.6	0.30±0.03	1.28±0.10

(2d) are for the majority of the processes very bad, and the cumulative χ^2 probabilities are very small. Moreover, the interpretation of the parameter α' in equation (2c) as a slope of a Regge trajectory is, in general, not possible.

4. *Regularities in the mass dependence of the slopes*

The cumulative χ^2 probability of hypothesis (2e) is significantly greater than the corresponding probabilities of the other hypotheses considered in this paper. However, looking at separate processes it is rather difficult to discriminate between parametrizations (2a) and (2e). The parameters entering equation (2e) exhibit, however, interesting regularities which may have some physical interpretation.

a) Behaviour at large masses — parameters b_0

Consider two processes in which production takes place at opposite vertices (Figs 3a and 3b, respectively). The sum of the limits b_0 is — within errors — equal to the value of the slope parameter in a related two-body or quasi two-body process (Fig. 3c) involving the "nonproduction" vertices of the processes represented by the diagrams in Figs 3a and 3b:

$$b^{(c)} = b_0^{(A)} + b_0^{(B)}. \tag{3}$$

Relation (3) is compared with the experimental data in Table V and represented graphically in Fig. 4. The values of the right-hand sides of relation (3) are indicated by the dashed horizontal lines and the corresponding errors by the shaded areas. The two-

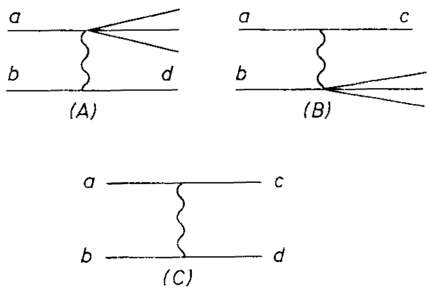

Fig. 3. Diagrams representing the processes involved in relation (3)

-body slopes are represented by full circles with error bars. Since formula (2e) contains three parameters, the comparison is presented only for those processes for which the number of the experimental points used in the fits is greater than four.

TABLE V

Comparison of relation (3) with experimental data

Left-hand side				Right-hand side				
Process	p_{lab}	Ref.	RHS	Vertex (A)	p_{lab}	Vertex(B)	p_{lab}	LHS
$\pi^+p \to \pi^+p$	8.0	[13]	8.0 ± 0.3	$\pi^+ \to \pi^{a}$	8.0	$p \to p$	8.0	7.1 ± 1.2
$\pi^-p \to \pi^-p$	16.0	[12]	8.3 ± 0.1	$\pi^- \to \pi^-$	16.0	$p \to p$	16.0	8.8 ± 1.1
$p\,p \to p\,p$	8.1	[9]	7.8 ± 0.5	$p \to p$	8.0	$p \to p$	8.0	9.5 ± 1.6
$p\,p \to p\,p$	10.9	[9]	9.0 ± 0.3	$p \to p$	10.1	$p \to p$	10.1	9.6 ± 0.6^{b}
$p\,p \to p\,p$	16.7	[9]	9.0 ± 0.4	$p \to p$	16.0	$p \to p$	16.0	10.8 ± 1.5
$p\,p \to p\,p$	19.2	[11]	8.8 ± 0.2	$p \to p$	19.2	$p \to p$	19.2	9.8 ± 1.2
$\pi^+p \to \pi^0\Delta^{++}$	8.0	[13]	7.5 ± 0.7	$\pi^+ \to \pi^{0\,c}$	8.0	$p \to \Delta^{++}$	8.0	6.7 ± 2.1
$K^+p \to K^0\Delta^{++}$	8.2	[15]	5.3 ± 1.0	$K^+ \to K^0$	8.2	$p \to \Delta^{++}$	8.0	5.2 ± 2.5
$K^-p \to \bar{K}^0n$	9.5/12.0	[14]	5.7 ± 0.8^{d}	$K^- \to \bar{K}^0$	10.1	$p \to n$	10.1	7.2 ± 1.1
$p\,p \to \Delta^{++}n$	8.1	[10]	10.5 ± 2.3	$p \to \Delta^{++}$	8.0	$p \to n$	10.1	10.8 ± 1.9
$p\,p \to \Delta^{++}\Delta^0$	8.1	[21]	7.3 ± 1.0	$p \to \Delta^{++}$	8.0	$p \to \Delta^0$	10.1	7.9 ± 1.8

[a] Process 11 in Table I. [b] Average value for processes 3 and 4 in Table I. [c] Process 18 in Table I.
[d] Average value for the two energies.

Table VI contains some predictions for the processes in which the two-body slope and one of the high-mass limits b_0 on the right-hand side of equation (3) are known.

In contrast to formula (2e) the parameters b_0 obtained using parametrization (2a) do not show any simple regularity.

b) Rates of decrease — parameters d

The rate of decrease towards the limiting value b_0 is determined in equation (2e) by parameter d (note, it has the dimension of the mass). As it is seen from Table IV the values of parameter d are rather similar for all the processes listed in the table: the values

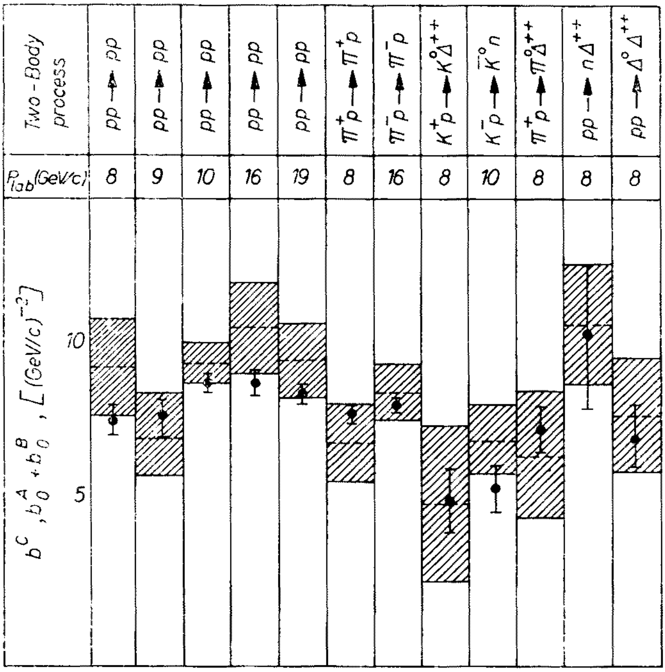

Fig. 4. Comparison of relation (3) with the experimental data. Horizontal dashed lines and the shaded areas represent the values and errors of the right-hand sides, respectively. Full circles with error bars represent the corresponding two-body and quasi two-body slopes

of d range only between 0.2 and 0.9 GeV. It is worth noting that even processes, for which the mass dependence of the slope looks quite different in Figs 2, have similar values of parameter d: *e.g.* processes 5 and 9 in Table I. This difference in steepness of the $b(M)$

TABLE VI

Predictions from relation (3)

Prediction			Input values				
Process	p_{lab} GeV/c	b_0 (GeV/c)$^{-2}$	Two-body channel	p_{lab} GeV/c	$b^{(c)}$ (GeV/c)$^{-2}$	Production process	b_0 (GeV/c)$^{-2}$
$K^-p \to K^-(p\pi^+\pi^-)$	10.1	2.9 ± 0.5	$K^-p \to K^-p$	10.1	7.7 ± 0.2	$K^-p \to p(K\pi)^-$	4.7 ± 0.3
$K^+p \to K^+(p\pi^+\pi^-)$	8.0	0.6 ± 1.0	$K^+p \to K^+p$	8.0	5.4 ± 0.2	$\pi^+p \to p(\pi^+\pi^+\pi)$	4.8 ± 0.8
$\pi^+p \to \pi_f^+(p\pi^+\pi^-)$	8.0	3.2 ± 0.9	$\pi^+p \to \pi^+p$	8.0	8.0 ± 0.3	$\pi^+p \to p(\pi^+\pi^+\pi^-)$	4.8 ± 0.8

The elastic scattering data are from references: [19] (K^-), [20] (K^+) and [13] (π^+).

plots for these two processes is due in equation (2e) to different values of parameter b_1 which determine the fitted values of the slope parameter at the threshold masses M_0.

c) Slopes at thresholds — parameters b_1

If factorization and gaussian formfactors are assumed, relation (3) suggests that the second term on the right-hand side of equation (2e) comes from the vertex at which system S is produced, whereas parameter b_0 determines the corresponding contribution from the "nonproduction" vertex. In this interpretation parameter b_1 can be considered as a contribution to slope at the threshold mass M_0 coming from the production vertex.

Table IV contains besides the values of b_1 also the values of $R = 2\sqrt{b_1}$. In the geometrical picture of high-energy scattering R can be associated with the radius of the hadron-hadron interaction. It is seen from Table IV that, in the majority of cases, R is roughly about 1 fm, which corresponds to the known radius of hadronic interactions. Parameters b_1 in equation (2a), which determine the slope parameter at $M_0 = 1$ GeV, do not seem to have any simple physical interpretation.

It is worth noting that the regularities described above concern both the inclusive and exclusive processes and, in the latter case, both the diffractive and nondiffractive channels. This would suggest that there exists some common ingredient in the mechanisms responsible for the decrease of the slope parameter in different kinds of production processes.

To summarize: the good χ^2 values and the regularities among the parameters favour strongly parametrization (2e) as compared to other parametrizations considered in this paper. Obviously, the particular shape of the gaussian fall-off towards the limit b_0 in equation (2e) is not very crucial here — rather, some more general features of parametrization (2e) should be emphasized:

i) with increasing mass $b(M)$ tends to a positive limit b_0 which is characteristic for the vertex at which production does not take place;

ii) the decrease towards this limit is rather fast and it can be well approximated by a gaussian function of the difference between the mass M of the produced system and the threshold mass M_0. The fall-off is faster than a logarithmic or power-law decrease[3];

iii) for $M \to M_0$, $b(M)$ increases rather slowly to a value $b(M_0) = b_1 + b_0$, where b_1 corresponds roughly to $R = 1$ fm through the geometrical relation: $b_1 = R^2/4$.

5. *Slopes at resonance masses*

As it can be seen from Figs 2a–2e the slopes at masses corresponding to resonances in system S deviate in some cases from smooth slope-versus-mass dependence of the neighbouring back-ground. The behaviour of slopes at the resonance masses is summarized in Table VII. The deviations from a smooth behaviour quoted in Table VII reffer to the best fit curves obtained using parametrization (2e). The errors correspond to the errors of the experimental points. Two features of the data in Table VII are worth noting:

[3] In Ref. [33] fits were performed to formulae (2a) and (2e) with the limits b_0 deduced from two-body and quasi two-body reactions through relation (3). The overall χ^2 probability of hypothesis (2a) is for those fits less than 0.05, whereas for hypothesis (2e) it is very good (about 0.5).

TABLE VII

Deviations from smooth slope-versus-mass dependence at resonance masses

Resonance	Q MeV	Process	Deviation $(\mathrm{GeV}/c)^{-2}$	Deviation in standard deviations
		Nondiffractive processes		
η	134	$\pi^+p \to (\pi^+\pi^-\pi^0)\Delta^{++}$	-2.2 ± 2.0	-1.1
K^*	258	$K^-p \to (K^0\pi^-)\,p$	-0.7 ± 0.3	-2.3
K^*	258	$K^-p \to (K^-\pi^+)\,n$	-2.9 ± 0.5	-5.8
K^*	258	$K^-p \to (K^0\pi^-)\Delta^+$	-2.6 ± 1.1	-2.4
K^*	258	$K^-p \to (K^-\pi^+)\Delta^0$	-2.4 ± 0.6	-4.0
ω	370	$\pi^+p \to \pi^+\pi^-\pi^0)\Delta^{++}$	-3.3 ± 1.3	-2.5
ϱ	486	$\pi^+p \to (\pi^+\pi^-)\Delta^{++}$	0.0 ± 0.5	0.0
K^{**}	774	$K^-p \to (K^0\pi^-)\,p$	$+0.4\pm0.6$	$+0.7$
K^{**}	774	$K^-p \to (K^-\pi^+)\,n$	0.0 ± 0.7	0.0
K^{**}	774	$K^-p \to (K^0\pi^-)\Delta^+$	$+0.6\pm1.1$	$+0.5$
K^{**}	774	$K^-p \to (K^-\pi^+)\Delta^0$	$+0.2\pm0.5$	$+0.4$
A_2	891	$\pi^+p \to (\pi^+\pi^-\pi^0)\Delta^{++}$	$+0.8\pm1.0$	$+0.8$
f^0	980	$\pi^+p \to (\pi^+\pi^-)\Delta^{++}$	$+2.2\pm0.8$	$+2.7$
		Diffractive processes		
Q	550	$K^-p \to (K^-\pi^+\pi^-)\,p$	-2.0 ± 0.6	-3.3
L	1000	$K^-p \to (K^-\pi^+\pi^-)\,p$	-0.1 ± 0.8	-0.1
A_2^a	891	$\pi^+p \to (\pi^+\pi^+\pi^-)\,p$	-2.1 ± 0.6	-3.3
A_2^b	891	$\pi^+p \to (\pi^+\pi^+\pi^-)\,p$	-1.9 ± 0.5	-3.8
A_2	891	$\pi^+p \to (\pi^-\pi^-\pi^+)\,p$	-2.2 ± 0.3	-7.3
A_1^a	660	$\pi^+p \to (\pi^+\pi^+\pi^-)\,p$	$+0.4\pm0.7$	$+0.6$
A_1^b	660	$\pi^+p \to (\pi^+\pi^+\pi^-)\,p$	-0.9 ± 0.7	-1.3
A_1	660	$\pi^-p \to (\pi^-\pi^-\pi^+)\,p$	-0.2 ± 0.5	-0.4
A_3^b	740	$\pi^+p \to (\pi^+\pi^+\pi^-)\,p$	$+0.3\pm0.7$	$+0.4$
A_3	740	$\pi^-p \to (\pi^-\pi^-\pi^+)\,p$	-0.4 ± 0.7	-0.6
ϱ	486	$\gamma p \to (\pi^+\pi^-)\,p$	0.0 ± 1.0	0.0

[a] at 16 GeV/c, [b] at 8 GeV/c.

a) In nondiffractive channels the deviations at resonance masses from a smooth behaviour are related to the Q-values of the resonances: the deviation increases with increasing Q-value, from negative at small Q (K^*, ω) to positive at large Q (f^0). This situation is illustrated in Fig. 5. The horizontal axis represents the Q-value of the resonance and the vertical one the deviation defined as above. The regularity illustrated by Fig. 5 suggests that the absence of any significant irregularities in the mass dependence of slopes at the ϱ and K^{**} masses is rather accidental and is related to the particular Q-values of these resonances.

b) In diffractive channels the slopes corresponding to resonance masses in mesonic systems deviate either towards smaller values of the slope (*e.g.* $Q(1320)$) or do not show any significant deviation (*e.g.* ϱ in photoproduction).

6. *Summary and conclusions*

Parametrization (2e) gives much better fits to the mass dependence of the slopes than other parametrizations proposed in the literature. It describes very well the data for both diffractive and nondiffractive exclusive channels, as well as the data for inclusive processes. The logarithmic decrease of the slope parameter predicted by a number of models (multi--regge, tripple-regge, Veneziano, thermodynamic) is shown to be inconsistent with the data when masses starting from near-threshold values are considered.

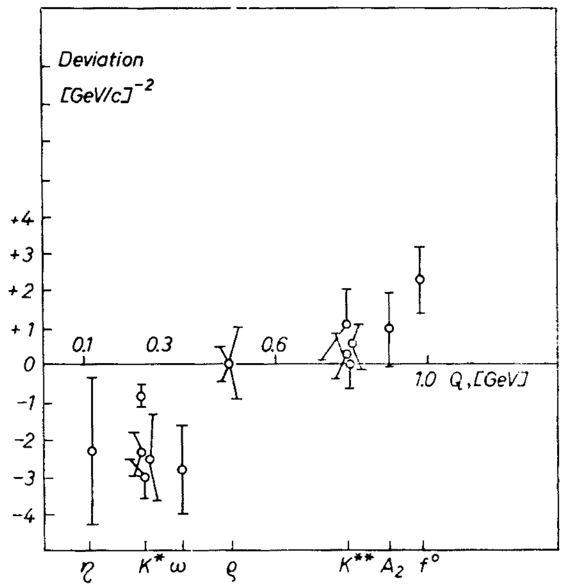

Fig. 5. Deviations at mesonic resonance masses in nondiffractive processes from a smooth behaviour of slope as a function of mass. The horizontal axis represents the Q-value of the resonance, ($Q = M - M_0$) and the vertical one the deviations from the best fit curves plotted in Figs 2a–2e

Additionally, parametrization (2e) exhibits interesting regularities in the data. These regularities are present in the data for different kinds of processes mentioned above, which indicates that the dominating mechanism responsible for the decrease of slope is similar in all production processes. Since the simple kinematical formula (2b) gives very bad fits to the data, it is rather likely that it is some dynamical mechanism. Relation (3) which connects the slopes at large masses in production processes to the slopes in two-body and quasi two-body reactions involving the relevant nonproduction vertices suggests that this mechanism should exhibit factorization, at least at large masses of the produced system. The decrease of slope with increasing mass could be then attributed to vanishing of the contribution to the slope coming from the form-factor of the vertex at which system S in Fig. 1 is produced.

The slopes at the masses corresponding to mesonic resonances produced in non-diffractive processes deviate from the best-fit curves obtained using parametrization (2e) in a way depending on the Q-value of the resonance: from negative deviatinons (*i.e.* towards smaller values of the slope) at small Q-values, to positive at the large ones (Fig. 5). The absence of significant deviations at resonances ϱ and K^{**} is, in view of this regularity, connected rather to the particular (intermediate) Q-values of these resonances and not to the similarity of the mechanisms responsible for the variation of the slope parameter with mass in the resonance and background production.

The author is indebted to Professor K. Zalewski, Professor A. Białas, Dr A. Bartke and Dr A. Eskreys for remarks and discussions.

REFERENCES

[1] J. Bartsch, M. Deutschmann, E. Keppel, G. Kraus, R. Speth, C. Grote, K. Lanius, S. Nowak, M. Walter, K. W. J. Barnham, H. Böttcher, V. T. Cocconi, J. D. Hansen, G. Kellner, A. Mihul, D. R. O. Morrison, V. I. Moskalev, K. Paler, H. Töfte, N. C. Barford, D. P. Dallman, N. C. Mukherjee, A. Frölich, W. Kittel, M. Markytan, G. Otter, *Phys. Lett.*, **27B**, 336 (1968).

[2] M. Deutschmann, R. Honecker, P. Schmitz, R. Speth, R. Steinberg, A. Meyer, E. Rysek, M. Walter, A. Angelopoulos, J. R. Campbell, V. T. Cocconi, G. Kellner, W. Kittel, D. R. O. Morrison, D. Sotiriou, R. Stroynowski, J. B. Whittaker, M. J. Counihan, P. J. Dornan, S. J. Goldsack, B. Buschbeck, M. Markytan, G. Otter, P. Schmid, *Nucl. Phys.*, **B36**, 373 (1972).

[3] K. Boesebeck, H. Grässler, G. Kraus, A. Schulte, H. Böttcher, J. Kaltwasser, K. Kaufmann, S. Nowak, K. Bockmann, M. Rost, J. G. Bossen, H. Drevermann, W. Johnssen, K. Sternberger, U. Stocker, A. Angelopoulos, J. R. Campbell, V. T. Cocconi, J. D. Hansen, W. Kittel, S. Matsumoto, D. R. O. Morrison, R. Stroynowski, J. B. Whittaker, J. Łoskiewicz, *Nucl. Phys.*, **B28**, 381 (1971).

[4] J. V. Beaupre, M. Deutschmann, H. Grässler, P. Schmitz, U. Gensch, W. D. Nowak, H. J. Schreiber, M. Walter, F. Grard, E. De Wolf, P. Herquet, L. Pape, P. Peeters, F. Verbeuere, R. Windmolders, A. Angelopoulos, P. V. Chliapnicov, V. T. Cocconi, O. Czyżewski, D. Drijard, P. Duinker, W. Dunwoodie, A. Eskreys, Y. Goldschmidt-Clermont, A. Grant, J. D. Hansen, V. P. Henri, W. Kittel, D. Linglin, S. Matsumoto, J. Meyer, D. R. O. Morrison, F. Muller, S. Nielsen, Z. Sekera, R. Stroynowski, P. J. Dornan, G. A. Grammatikakis, B. R. Kumar, A. Mutalib, B. Buschbeck, A. Froehlich, P. Porth, H. Wahl- *Nucl. Phys.*, **B30**, 381 (1971).

[5] W. Kittel, S. Ratti, L. Van Hove, Aachen—Berlin—Bonn—CERN—Cracow—Heidelberg—Warsaw and Genova—Hamburg—Milano—Saclay Collaborations, *Nucl. Phys.*, **B30**, 333 (1971).

[6] S. Ljung, H. I. Miettinen, R. O. Raitio, J. Tuominiemi and The Scandinavian Bubble Chamber Collaboration; *Study of the 1470 and 1710 Enhancements in the Reaction $pp \to p\pi^-\Delta^{++}$ at 19 GeV/c*, paper submitted to the Colloquium on Multiparticle Dynamics, Helsinki 1971.

[7] P. K. Schilling, DESY Int. Report R1/70/3, (1970).

[8] J. Bartsch, G. Kraus, R. Speth, L. Azhgirey, U. Gensch, J. Klugow, H. J. Schreiber, T. Besliu, J. R. Campbell, V. T. Cocconi, P. Duinker, G. Kellner, W. Kittel, D. R. O. Morrison, R. Stroynowski, S. J. Goldsack, G. Grammatikakis, B. R. Kumar, M. J. Losty, B. Buschbeck-Czapp, M. Markytan, P. Schmid, H. Wahl, *Nucl. Phys.*, **B40**, 103 (1972).

[9] Kh. M. Chernov, *On the Slope Parameter of the Elastic $p-p$ Scattering Differential Cross Section*, Dubna preprint, P1-6358 (1972), in Russian.

[10] O. Benary, L. R. Price, G. Alexander, *NN and ND Interactions above 0.5 GeV/c — A Compilation*, UCRL-20000 NN (1970).

[11] J. V. Allaby, F. Binon, A. N. Diddens, P. Duteil, A. Klovning, R. Meunier, J. P. Peigneux, E. J. Sacharidis, K. Schlupmann, M. Spighel, J. P. Stroot, A. M. Thorndike, A. M. Wetherell, *Phys. Lett.*, **28B**, 67 (1968).
[12] R. Honecker, B. Junkmann, R. Schulte, R. Steinberg, N. Tsanos, J. Klugow, S. Nowak, E. Ryseck, M. Walter, K. Böckmann, H. Drevermann, W. Johnssen, K. Sternberger, H. Böttcher, V. T. Cocconi, J. D. Hansen, G. Kellner, D. R. O. Morrison, K. Paler, A. Mihul, V. Moskalev, T. Coghen, O. Czyżewski, K. Eskreys, J. Łoskiewicz, J. Zaorska, S. Brandt, O. Braun, V. Luth, T. P. Shah, H. Wenninger, M. Bardadin-Otwinowska, T. Hofmokl, L. Michejda, W. Wójcik, S. Otwinowski, R. Sosnowski, M. Szeptycka, A. Wróblewski, *Nucl. Phys.*, **B13**, 571 (1969).
[13] M. Aderholz, M. Deutschmann, E. Keppel, G. Kraus, H. Weber, C. Grote, H. H. Kaufmann, S. Nowak, M. Walter, H. Böttcher, T. Byer, V. T. Cocconi, P. F. Dalpiaz, J. D. Hansen, G. Kellner, W. Kittel, M. Markytan, A. Mihul, D. R. O. Morrison, H. Töfte, *Nucl. Phys.*, **B8**, 45 (1968).
[14] P. Astbury, G. Brautti, G. Finocchiaro, A. Michelini, K. Terwilliger, D. Websdale, C. H. West, P. Zanella, W. Beusch, W. Fischer, B. Gobbi, M. Pepin, E. Polgar, *Phys. Lett.*, **23**, 396 (1966).
[15] W. De Baere, J. Debaisieux, P. Dufor, F. Grard, J. Heughebauert, L. Pape, P. Peeters, F. Verbeure, R. Windmolders, G. Bassompierre, D. Drijard, Y. Goldschmidt-Clermont, A. Grant, V. P. Henri, B. Jongejans, D. Linglin, F. Muller, J. M. Perreau, H. Piotrowska, I. Saitov, R. Sekulin, G. Wolf, *K^* and N^* Production in the $K^0p\pi^+$ Final State at K^+ Incoming Momenta from 3 to 8.25 GeV/c*, paper presented at the International Conference on High Energy Physics, Vienna 1968.
[16] H. Satz, *Phys. Lett.*, **32B**, 380 (1970).
[17] A. Guła, *Nuovo Cimento Lett.*, **7**, 63 (1973).
[18] H. Muirhead, *The Mass Dependence of the Slopes in High Energy Scattering*, preprint (1971).
[19] M. Aderholz, M. Deutschmann, E. Keppel, G. Kraus, H. Weber, U. Gensch, G. Grote, S. Nowak, D. Pose, H. Böttcher, T. A. Byer, V. T. Cocconi, E. Flaminio, J. D. Hansen, G. Kellner, U. Kruse, J. Łoskiewicz, M. Markytan, D. R. O. Morrison, N. C. Barford, D. P. Dallman, S. J. Goldsack, N. C. Mukherjee, W. Kittel, C. Kraft, D. Khun, G. Otter, I. Wacek, *Nucl. Phys.*, **B7**, 111 (1968).
[20] C. Y. Chien, E. Malamud, D. J. Mellema, P. E. Schlein, W. E. Slater, D. H. Stork, H. K. Ticho, *Phys. Lett.*, **28B**, 615 (1969).
[21] G. Kayas, J. Le Guyader, M. Sene, T. P. Yion, J. Alitti, Nguen Thuc Diem, G. Smadja, J. Gingest, D. Manesse, Tran Ha Ah, *Nucl. Phys.*, **B5**, 169 (1968).
[22] J. Ballam, G. B. Chadwick, Y. Eisenberg, E. Kogan, K. C. Moffeit, P. Seyboth, I. O. Scillicorn, H. Spitzer, G. Wolf, H. H. Bingham, W. B. Fretter, W. J. Podolsky, M. S. Rabin, A. H. Rosenfeld, G. Smadja, *Vector Meson Production by Polarised Photons at 2.8, 4.7, and 9.3 GeV*, preprint SLAC-PUB-1143, LBL-1371 (1972).
[23] Aachen—Berlin—Bonn—CERN—Heidelberg Collaboration, paper submitted to the XVI International Conference on Elementary Particles in Batavia (1972).
[24] W. E. Ellis, R. R. Kinsey, T. W. Morris, R. S. Panvini, F. Turkot, *Phys. Lett.*, **32B**, 641 (1970).
[25] W. E. Ellis, T. W. Morris, R. S. Panvini, F. Turkot, *Peripheral Processes in Proton-Proton Interaction at 29 GeV/c*, preprint BNL 13918 (1969).
[26] W. E. Ellis, T. W. Morris, R. S. Panvini, A. M. Thorndike, *A Description of Final States with Three, Four, and Five Particles in pp Interactions at 28.5 GeV/c*, preprint BNL 13671 (1969), paper submitted at the Lund International Conference on Elementary Particles in Lund, 1969.
[27] J. Trefil, *Nuovo Cimento*, **63A**, 961 (1969).
[28] L. Caneschi, *Nuovo Cimento Lett.*, **4**, 122 (1969).
[29] See *e.g.*, K. Gottfried, *An Introduction to Multiple Production Processes*, lectures, preprint Ref. TH. 1615-CERN (1973).

[30] L. N. Chang, P. G. O. Freund, Y. Nambu, *Phys. Rev. Lett.*, **24**, 628 (1970).
[31] R. Blutner, Htun Than, E. Matthaus, G. Ranft, J. Ranft, *Nucl. Phys.*, **B35**, 503 (1971).
[32] C. E. DeTar, Kuyngsik Kang, C. I. Tan, J. H. Weis, *Phys. Rev.*, **D4**, 425 (1971); D. Gordon, G. Veneziano, *Phys. Rev.*, **D3**, 2116 (1971).
[33] A. Guła, *Possible Parametrization of the Mass Dependence of Slope in Production Processes*, paper submitted to the III International Colloquium on Multiparticle Reactions in Zakopane, 1972.